Time Domain Modeling for Large Scale Cosite Interference Problems Utilizing Parallel Computing and Wavelets

Costas D. Sarris[1], Pawel Czarnul[1], Donghoon Chun[1],
Karen Tomko[2], Edward S. Davidson[1], Linda P. B. Katehi[1]
and Barry Perlman[3]

[1] Department of Electrical Engineering and Computer Science, University of Michigan, Ann Arbor
[2] Department of Electrical and Computer Engineering and Computer Science, University of Cincinnati
[3] CECOM RDEC, I2WD, Ft. Monmouth, NJ.

Abstract

The rigorous electromagnetic modeling of cosite interefence between neighboring vehicular transceivers is pursued in this paper. In particular, Maxwell's equations are solved in the time domain for the full wave modeling of wave propagation, along with state equations, descriptive of the operation of front-end transceiver electronics. Hence, a combined electromagnetic and circuit modeling, that allows for the complete characterization of nonlinear effects pertinent to cosite interefence phenomena, is presented. Since the use of conventional techniques such as the Finite Difference Time method for the treatment of such problems typically results in long, computationally burdensome simulations the use of wavelet based time domain solvers combined with parallelization techniques is proposed.

I. Introduction

With the recent advances in mobile communications and their growing use in commercial and military applications, the rigorous analysis of electromagnetic intereference (EMI) between antennas mounted on neighboring platforms has become a topic of critical importance. In particular, the concurrent operation of transceiver systems in proximity with each other and their resultant parasitic reception of interfering signals, can cause a number of unwanted effects, potentially driving system power amplifier stages to saturation, the well - known effect of desensitization that can even block the operation of radio networks [1], or creating intermodulation products that ultimately undermine the overall system performance. For the complete theoretical characterization of such effects and the physical understanding of their phenomenology, the integrated modeling of both electromagnetic wave propagation across a given communication channel and the wave interaction with transceiver front-end electronics is motivated.

For this dual purpose, time domain techniques such as the Finite Difference Time Domain (FDTD, [5]) are well suited for two reasons: First, FDTD offers a mathematically straightforward and inherently versatile method for the analysis of arbitrary electromagnetic geometries. In this sense, FDTD serves a major objective of our study well, that being to capture the effect of the platforms on the radiative properties of the antennas that are mounted on them. Second, it was recently demonstrated that the incorporation of active element components and nonlinear circuits in the FDTD mesh can be easily accomplished by following a state equation based approach [2]. Hence, the simulation of nonlinear effects pertinent to cosite interference is made possible.

However, as FDTD is a second order accurate scheme, and sensitive to numerical dispersion, a dense discretization of at least ten, but usually twenty five points per wavelength is necessary for the extraction of a convergent solution. Thus, the FDTD treatment of electrically large domains corresponding to geometries of cosite vehicular transceivers (even in VHF band operation), yields a computationally intensive, memory and execution time consuming calculation.

For the alleviation of the computational burden involved in FDTD simulations, this paper follows two directions of research. The first is the use of parallelization for the distributed update of the electromagnetic field values in the computational domain over several processors, while the second is the introduction of wavelets for the implementation of a space and time adaptive gridding via the Multiresolution Time Domain (MRTD) technique [3]. The Haar wavelet basis is employed, for the reason that its update equations include only nearest neighbor interactions, in contrast with higher order basis functions, whose stencil extends over several cells. Thus, the Haar basis is considered as a promising candidate for the application of parallel computing to MRTD.

In the following, the aforementioned modeling approach is explained in greater detail and numerical results regarding typical problems that this work aims to address are provided.

Research supported by the Army Research Office / CECOM under the project for "Efficient Numerical Solutions to Large Scale Tactical Communication Problems" (DAAD19-00-1-0173).

II. The Three Dimensional FDTD / Haar MRTD Scheme

A. Concept

The MRTD technique assumes an expansion of field quantities in a multilevel level basis of *scaling* ϕ and *wavelet* ψ functions of the form :

$$f(x) = \sum_k c_k \, \phi(x-k) \; + \; \sum_k \sum_j d_{j,k} \, \psi\left(2^j x - k\right) \tag{1}$$

where the coefficients $\{c_k\}$ and $\{d_k\}$ represent the multiresolution decomposition of the function f. In particular, the scaling coefficients $\{c_k\}$ represent mean field values at the $k-$th cell, while wavelet coefficients $\{d_k\}$ roughly correspond to field derivatives and assume significant values at regions of high field variations. Therefore, thresholding of wavelet coefficients (that is elminating them from subsequent operations if their value is below a certain accuracy-related threshold) leads to the establishment of an effectively adaptive, moving mesh, dynamically arranged by the wavelet values themselves. This straightforward implementation of adaptive gridding, that MRTD allows for, motivates its application to large scale problems.

B. Formulation

The three dimensional Haar wavelet based MRTD scheme is formulated in this section. For this purpose, all electric and magnetic field components are expanded in Haar scaling and wavelet functions $\phi_{\,m}(\xi) = \phi(\xi - m)$, $\psi^r_{m,p}(\xi) = 2^{r/2}\,\psi\left(2^r(\xi-m)-p\right)$, in all directions $\xi = x,\ y,\ z$, with $r = 0, 1 \cdots r_{max}$ being an index denoting the resolution of the wavelet term (varying from 0 to r_{max}) and $p(r) = 0, 1, \cdots 2^r - 1$ being a counter of the r-order wavelets within each cell. The Haar scaling and mother wavelet functions are depicted in Fig. 1.

It is noted that the introduction of one wavelet level (zero order) in x, y, z - directions is expected to bring about an improvement in resolution of a factor of two per direction (hence, eight in total) compared to a scaling only based scheme. However, for this to be true, a certain condition regarding the arrangement of electric and magnetic field nodes need be imposed, as discussed in [4]. Namely, as the offset of electric and magnetic field nodes is half a cell in FDTD, in an $r-$order Haar MRTD (of $r+1$ - wavelet levels) this offset must be set equal to one cell by 2^{r+2}. For example, the E_x component of the electric field is expanded as :

$$\begin{aligned}
E_x(\overline{r},t) \;=\; & \sum_n h_n(t) \sum_{i,j,k} \Bigg\{ {}_nE^{\phi\,\phi\,\phi}_{i',j,k}\phi_{i'}(x)\phi_j(y)\phi_k(z) + \sum_{r_z,p_z} {}_nE^{\phi\,\phi\,\psi_{r_z,p_z}}_{i',j,k}\phi_{i'}(x)\phi_j(y)\psi^{r_z}_{k,p_z}(z) \\
& + \sum_{r_y,p_y} \Bigg\{ {}_nE^{\phi\,\psi_{r_y,p_y}\,\phi}_{i',j,k}\phi_{i'}(x)\psi^{r_y}_{j,p_y}(y)\phi_k(z) + \sum_{r_z,p_z} {}_nE^{\phi\,\psi_{r_y,p_y}\,\psi_{r_z,p_z}}_{i',j,k}\phi_{i'}(x)\psi^{r_y}_{j,p_y}(y)\psi^{r_z}_{k,p_z}(z) \Bigg\} \\
& + \sum_{r_x,p_x} \Bigg\{ {}_nE^{\psi_{r_x,p_x}\,\phi\,\phi}_{i',j,k}\psi^{r_x}_{i',p_x}(x)\phi_j(y)\phi_k(z) + \sum_{r_z,p_z} {}_nE^{\psi_{r_x,p_x}\,\phi\,\psi_{r_z,p_z}}_{i',j,k}\psi^{r_x}_{i',p_x}(x)\phi_j(y)\psi^{r_z}_{k,p_z}(z) \Bigg\} \\
& + \sum_{r_x,p_x,r_y,p_y} \Bigg\{ {}_nE^{\psi_{r_x,p_x}\,\psi_{r_y,p_y}\,\phi}_{i',j,k}\psi^{r_x}_{i',p_x}(x)\psi^{r_y}_{j,p_y}(y)\phi_k(z) + \sum_{r_z,p_z} {}_nE^{\psi_{r_x,p_x}\,\psi_{r_y,p_y}\,\psi_{r_z,p_z}}_{i',j,k}\psi^{r_x}_{i',p_x}(x)\psi^{r_y}_{j,p_y}(y)\psi^{r_z}_{k,p_z}(z) \Bigg\} \Bigg\}
\end{aligned} \tag{2}$$

where $i' \equiv i + 1/2^{rx,max+2}$, $r_{x,max}$ denotes the maximum wavelet order in $x-$direction and $h_{\,n}$ are the pulse functions defined in [3]. The rest of the EM field components are accordingly defined. The combination of scaling and wavelet terms yields equivalent grid points whose arrangement (under the condition followed here) in the equivalent Yee's cell of MRTD is shown in Fig. 2, where $\rho_\xi = 2^{r_{\xi,max}+1}$, $\xi = x, y, z$ (refinement factor). Finally, a dispersion analysis of this scheme shows that its dispersion characteristics are given by the expression :

$$\left\{\frac{1}{u_p\Delta t}\,\sin\frac{\omega\Delta t}{2}\right\}^2 = \left\{\frac{1}{\Delta x_{eff}}\sin\frac{k_x\,\Delta x_{eff}}{2}\right\}^2 + \left\{\frac{1}{\Delta y_{eff}}\sin\frac{k_y\,\Delta y_{eff}}{2}\right\}^2 + \left\{\frac{1}{\Delta z_{eff}}\sin\frac{k_z\,\Delta z_{eff}}{2}\right\}^2 \tag{3}$$

where $\Delta x_{eff} = \Delta x/2^{r_{x,max}+1}$, $\Delta y_{eff} = \Delta y/2^{r_{y,max}+1}$, $\Delta z_{eff} = \Delta z/2^{r_{z,max}+1}$ and Δx, Δy, Δz are the scaling cell sizes. Equation (3) shows that the formulated Haar MRTD scheme is dispersionwise equivalent to a Yee's scheme of cell sizes $\Delta x_{eff},\ \Delta y_{eff}, \Delta z_{eff}$.

The rest of our derivation follows the Method of Moments based technique that is set forth in [3].

III. Cosite Interference Problem Modeling

A. Geometry / Open boundaries

The general form of cosite interference scenarios considered in this work, is shown in Fig. 3 which depicts two neighboring vehicular tranceivers. Cases of more vehicular tranceivers or multiple antennas mounted on the same platform are also considered.

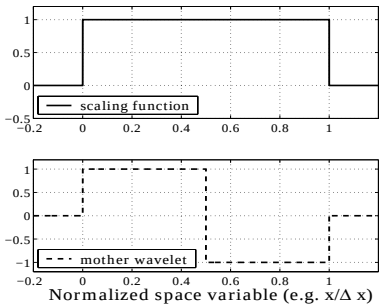

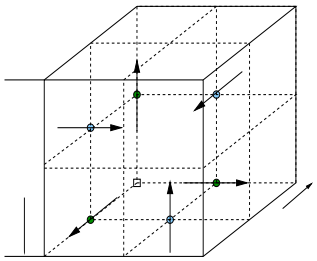

Fig. 1. Haar scaling and mother wavelet functions.

Recognizing the terms on the right handside of (4) as the device current and the displacement current respectively, giving rise to a total Norton equivalent current I_N, the equivalent circuit of Fig. 5 is extracted. Thus, Ampere's law takes on the equivalent form of Kirchhoff's current law :

$$I_N(t) = I_{dev}(t) + C_N \frac{d}{dt} V_{dev}(t), \tag{5}$$

where $C_N = \epsilon_0 \, \Delta y \, \Delta z / \Delta x$ denotes the equivalent capacitance of the FDTD cell.

C. Parallelization

The parallel FDTD algorithm currently uses a static regular block based partitioning strategy in which each processor is assigned one block of the domain to work on. The computational workload is non-uniform across the domain with little or no computation performed for cells within a vehicle and additional computations for cells within the absorber regions. The partitioning strategy uses relative computational weights for each type of cell to adjust the subdomain boundaries and compensate for this imbalance. The MPI library is used for communication between processors owning neighboring cells.

IV. Numerical Results

The vehicle model that is used in our simulations is shown in Fig. 6. The vehicle trunk is considered as a perfect electric conductor, an assumption that is valid in the VHF band. The vehicle antenna is modeled as a monopole mounted on the rear part of the platform. Two case studies are presented here, including two neighboring vehicular tranceivers in hybrid operation (one of them is in transmit and the other in receive mode). This operation is simulated by using a transparent, 0-0.6 GHz Gaussian excitation at the gap of the "active" antenna. For the derivation of the following results, the FDTD method was applied, with Yee's cell dimensions being equal to 5 cm by 5 cm by 5 cm. The receiving antenna was terminated at a parallel RLC block with $R = 1 \; K\Omega$, $L = 1 \; \mu H$, $C = 10 \; pF$, that was modeled by means of the earlier explained state equation approach of [2]. It is noted that the antennas were $x-$ directed and considered as one cell thick and one meter long. Local subgridding techniques can be readily employed for the modeling of thinner monopoles. Finally, the time step was equal to 92 $psec$. For the execution of parallel runs, the NPACI Blue Horizon teraflop-scale Power3 based clustered SMP system is used. The system has 1152 processors, 512GB memory which are arranged as 144 SMP nodes each with 8 375MHz Power3 processors and 4GB memory shared among them. Timing measurements correspond to 100 time-step runs, each being executed 3 times. Both average and minimum times are shown.

The first geometry under study is depicted in Fig. 7 and yields a relatively large working volume of 70 by 274 by 204 cells terminated into 10 UPML cells at each open boundary. Input current waveforms for the two antennas (derived by means of Ampere's law) are shown in Fig. 8. Even the apparently weak coupling between the two antennas can adversely affect the receive operation of the second and its sensitivity to signals coming from remote transmitters, when the spectral content of the interfering signal is within the bandwidth of the input stage filter of the receiver [1]. For the validation of the active element modeling, the input impedance of the receiver is computed, by Fourier transforming the time domain input voltage and current data of 8192 time steps. The resulting pattern of the parallel RLC combination is thus derived and compared successfully to its theoretical value (Fig. 9). Parallelizing the code, speed-ups of more than 90 were obtained on 128 processors (Fig. 10). Timing measurements for the same case are given in Fig. 11.

A second case study is shown in Fig. 12. Again, antenna 1 is considered as a transmitter, while antenna 2 is loaded by a parallel RLC block, being in receive mode. The input current waveform at antenna 1 is almost identical to the one of the previous case (only differning at some low amplitude retro-reflections). Input current and voltage waveforms for antenna 2 are given in Fig. 13. Furthermore, Fig. 14 includes three snapshots of E_x at time steps 400, 800, 1200 sampled at a $z-$ plane that includes the transmitting antenna, clearly showing the metal trunks of the vehicles and the free space propagation of the excitation pulse that is emitted from the transmitter and eventually covers the whole space, illuminating the second vehicle. Finally, for this case, speedup of more than 85 was obtained on 128 processors (Fig. 15). Execution time measurements are also shown in Fig. 16.

V. Conclusions

A research effort to rigorously model cosite interference problems by time domain methods such as FDTD and MRTD, combined

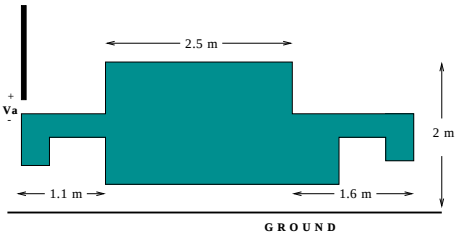

Fig. 6. Vehicle model.

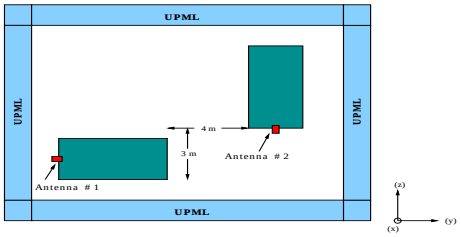

Fig. 7. Computational domain for the first cosite interference scenario ($yz-$ plane).

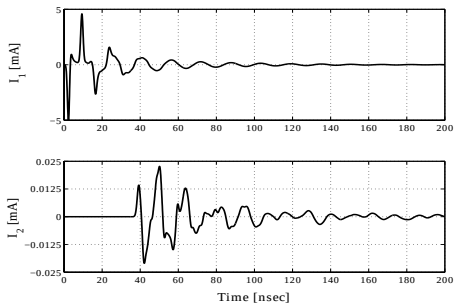

Fig. 8. Input currents for the two antennas of Fig. 7.

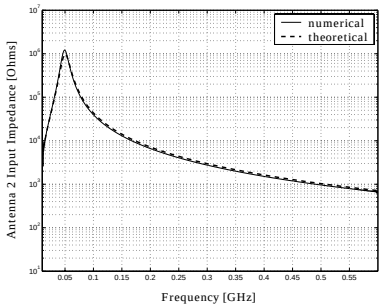

Fig. 9. Numerical and theoretical value of the input impedance of antenna 2 (Fig.7).

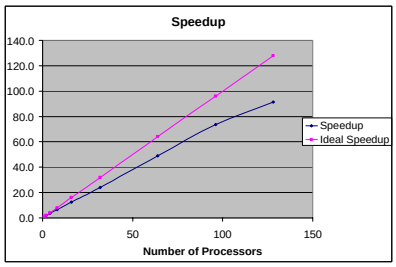

Fig. 10. Parallel speed-up curve for the geometry of Fig. 7.

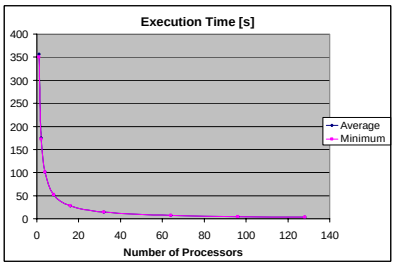

Fig. 11. Execution time with respect to processors for the geometry of Fig. 7.

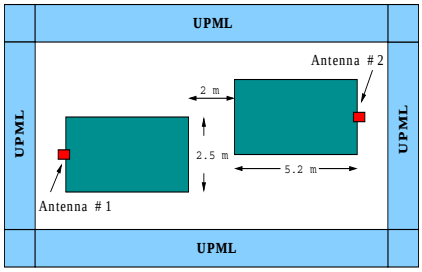

Fig. 12. Computational domain for the second cosite interference scenario ($yz-$ plane).

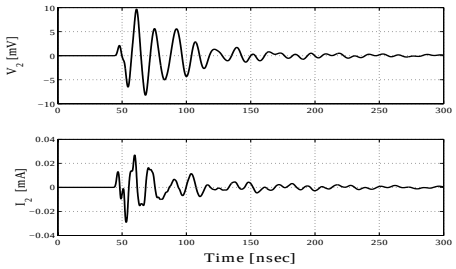

Fig. 13. Input voltage and current of antenna 2 of Fig. 12.

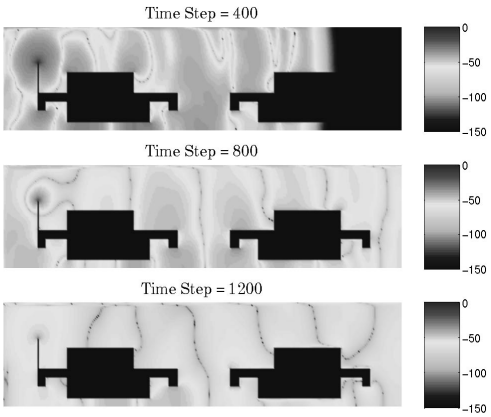

Fig. 14. E_x field pattern sampled at the $z-$plane containing antenna 1 in the geometry of Fig.12.

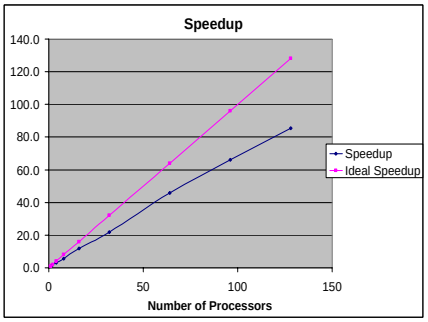

Fig. 15. Parallel speedup curve for the geometry of Fig. 12.

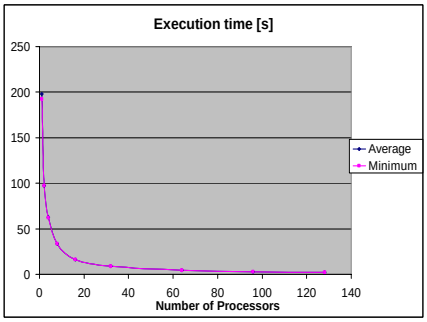

Fig. 16. Execution time with respect to processors for the geometry of Fig. 12.

[2] B. Houshmand, T. Itoh, M. Picket-May, "High-Speed Electronic with Active and Nonlinear Components", *ch. 8, in Advances in Computational Electrodynamics, the Finite Difference Time Domain Method, A. Taflove ed., Artech House, Boston, 1999.*

[3] M. Krumpholz, L.P.B. Katehi, "MRTD: New Time Domain Schemes Based on Multiresolution Analysis", *IEEE Trans. Microwave Theory and Techniques, vol.44, no.4, pp.555-561, April 1996.*

[4] C. D. Sarris, L. P. B. Katehi, "Fundamental Gridding Related Dispersion Effects in Multiresolution Time Domain Schemes", *Proceedings of the 2001 IEEE International Microwave Symposium.*

[5] K. S. Yee, "Numerical solution of initial boundary value problems involving Maxwell's equations in isotropic media ", *IEEE Trans. Antennas Prop., vol. 14, no. 3, pp. 302-307, March 1966.*

[6] S. Gedney, "The Perfectly Matched Layer Absorbing Medium", *ch. 5 in* Advances in Computational Electrodynamics : The Finite Difference Time Domain Method, *A. Taflove, ed.*, Artech House, 1998.

[7] C. D. Sarris, L. P. B. Katehi, "Development and Application of an Efficient FDTD/MRTD Numerical Interface", *accepted for presentation in the 2001 IEEE International Microwave Symposium.*

[8] R. L. Robertson, C. D. Sarris, L. P. B. Katehi, "Analysis of Lumped Element Transistor Structures Using MRTD : The State Equation Approach", *submitted to the IEEE Microwave and Guided Wave Letters, October 2000.*

[9] C.D. Sarris, K. Tomko, P. Czarnul, S.H. Hung, R.L. Robertson, D. Chun, E.S. Davidson, L. P. B. Katehi, "Multiresolution Time Domain Modeling for Large Scale Wireless Communication Problems", *accepted for presentation in the 2001 IEEE AP-S International Symposium on Antennas and Propagation.*